BEC preprints

BEC preprints 2025.7
https://doi.org/10.26124/becprep.2025-0007

Open Access

Technical Communications

Cite
Cecatto C, Cardoso LHD, Grings M, Gnaiger E (2025) Mitochondrial Ca^{2+} uptake and high-resolution respirometry. BEC preprints 2025.7. https://doi.org/10.26124/becprep.2025-0007

Author contributions
Conceptualization: CC, EG
Data curation, formal analysis, methodology: CC, LHDC, EG
Investigation: CC
Project administration, resources, supervision, validation: EG
Visualization, writing original draft: CC, LHDC, EG
Review and editing: CC, LHDC, MG, EG
All authors wrote the manuscript.

Conflicts of interest
CC, LHDC, and MG are employees of Oroboros Instruments. EG is founder and CEO of Oroboros Instruments.

Received 2025-07-16
Accepted 2025-07-16
Published 2025-07-17

Data availability
Data available Open Access https://doi.org/10.5281/zenodo.15754082

Keyword
calcium;
mitochondria;
mitochondrial permeability transition pore;
calcium green;
high-resolution respirometry.

Mitochondrial Ca^{2+} uptake and high-resolution respirometry

Cristiane Cecatto, Luiza Helena Daltro Cardoso, Mateus Grings, Erich Gnaiger

Oroboros Instruments GmbH, Innsbruck, Austria
Corresponding authors: cristiane.cecatto@oroboros.at; erich.gnaiger@oroboros.at

Summary

Mitochondrial calcium homeostasis is involved in the regulation of calcium-dependent cellular processes. Mitochondria contribute to the buffering of cytosolic free calcium levels by uptake and release, or storage of osmotically inactive calcium phosphates in the mitochondrial matrix. Defective calcium homeostasis is a cause of bioenergetic stress, cell death, and diseases. Frequently, calcium retention capacity is measured as the amount of calcium titrated up to a threshold, when calcium uptake is reversed and permeability transition triggers the release of calcium, disruption of ion balance, dyscoupling, and inhibition of respiration. This is accompanied by leakage into the cytosolic space of signaling molecules such as cytochrome *c*. Since the interplay between mitochondrial Ca^{2+} uptake and oxidative phosphorylation is well recognized, an advanced integrated methodology to concurrently assess mitochondrial respiration and Ca^{2+} dynamics has the potential to enhance our understanding of their crosstalk under physiological and pathological conditions. Here, we present an optimized protocol for the simultaneous measurement of extramitochondrial Ca^{2+} using Calcium Green™-5N (CaG) in conjunction with high-resolution respirometry. We identified MiRCa medium containing CaG as suitable for concurrent assays without impairing respiration of isolated mouse liver mitochondria. A standardized Ca^{2+} calibration protocol was developed. This integrated assay enables real-time monitoring of mitochondrial Ca^{2+} handling and bioenergetic function, offering a valuable tool for exploring mitochondrial function in health and disease.

1. Introduction

Mitochondria are central to cellular bioenergetics, primarily through their role in oxidative phosphorylation (OXPHOS). Beyond energy transformation, they play a crucial role in maintaining cellular calcium homeostasis by sequestering cytosolic calcium ions (Ca^{2+}). Ca^{2+} is a pivotal and ubiquitous second messenger in various cellular signaling pathways (Berridge et al 2000; Clapham 2007; Modesti et al 2021). Mitochondrial Ca^{2+} homeostasis is linked to cell survival and cell death. Excessive mitochondrial Ca^{2+} accumulation initiates apoptosis, necrosis, or autophagy (Duchen 2004; Giorgi et al 2018). At lower concentrations, Ca^{2+} activates pyruvate dehydrogenase phosphatase, oxoglutarate dehydrogenase, NAD-isocitrate dehydrogenase, FAD-glycerol phosphate dehydrogenase, and F1-FO-ATPase (McCormack et al 1990; Balaban 2009; Denton, 2009), but the impact on oxidative phosphorylation depends on the concentration of Ca^{2+} (Vinnakota et al 2011; Vilas-Boas et al 2023).

Upon cell stimulation by diverse mechanisms (for a review see Berridge et al 2000), Ca^{2+} is released from intracellular stores in the endoplasmic or sarcoplasmic reticulum (ER/SR). After the signaling event the Ca^{2+} is removed from the cytoplasm, with mitochondria playing a central role in maintaining cellular Ca^{2+} homeostasis (Marchi, Pinton 2014; Carvalho et al 2020). Pathological conditions can lead to Ca^{2+} cell overload, which is potentially lethal to the cell if not properly regulated.

Ca^{2+} uptake through the mitochondrial outer membrane is mediated by the voltage-dependent anion channel (VDAC), while the transport across the mitochondrial inner membrane (mtIM) is primarily mediated by the mitochondrial calcium uniporter (MCU) (De Mario et al 2023; Duvvuri, Lood 2021). Transport via the MCU is electrogenic, driven by the mitochondrial membrane potential (mtMP) (Giorgi et al 2018). The balance of matrix Ca^{2+} concentration is maintained by Ca^{2+} antiporters, including the mitochondrial $Na^{+}/Ca^{2+}/Li^{+}$ exchanger (NCLX) and the H^{+}/Ca^{2+} exchanger (HCX), depending on tissue type (Modesti et al 2021).

Once inside the mitochondria Ca^{2+} forms phosphate-precipitates, but excessive uptake or impairment of the efflux system causes a massive Ca^{2+} release upon opening of the mitochondrial permeability transition pore (mtPTP) (Carraro, Bernardi 2023). Transient or prolonged opening leads to mtIM depolarization and mitochondrial swelling, and inducing cell death (reviewed by Modesti et al 2021). Besides Ca^{2+} as an essential permissive agent for pore opening, the mtPTP is controlled by the protonmotive force and desensitized by Cyclosporin A (CsA) (Bernardi et al 2015). The structure of the mtPTP is a matter of debate. There is good evidence for regulatory and/or structural roles of the adenine nucleotide translocator, F-ATP synthase and Cyclophilin D (Bernardi et al 2023). Several proteins — such as phosphate carrier, VDAC, and hexokinase — act as modulators of its function. Multiple forms of mtPTP may exist with different molecular composition, depending on the conductance of the pore (low vs. high) (Endlicher et al 2023).

The Ca^{2+} movements can be easily measured using a Ca^{2+} fluorescent probe. A widely applied method uses the visible light-excitable Ca^{2+} indicator Invitrogen™ Calcium Green™-5N (CaG), which is a membrane-impermeant potassium salt and therefore can be dissolved in water. It has lower buffering capacity for intracellular Ca^{2+} compared to high-affinity dyes. In assays with isolated mitochondria, it enables to investigate the extramitochondrial Ca^{2+} concentration, and it is ideal for tracking rapid Ca^{2+}-release kinetics (Thermo Fischer Scientific 2010).

While CaG is commonly used in spectrofluorimetry to study Ca^{2+} homeostasis, its application in simultaneous assessments of mitochondrial respiration and calcium dynamics warrants further exploration. Monitoring mitochondrial respiration simultaneously to Ca^{2+} uptake and retention/release may advance the understanding of how Ca^{2+} (dys)homeostasy impacts energy metabolism. The composition of incubation media greatly affects calcium uptake capacity (CaUC) or the so-called calcium retention capacity (CaRC), complicating comparison between studies (Endlicher et al 2023). Standardization of the method and nomenclature are needed.

Despite the critical interplay between mitochondrial calcium uptake and respiration, few studies have simultaneously measured these parameters (Nászai et al 2019; Spinazzi et al 2019; Deline et al 2021; Ahn et al 2022; Xu et al 2022; Donnelly et al 2024). Addressing this gap, we introduce a method to concurrently assess mitochondrial Ca^{2+} dynamics and respiratory function.

This paper describes a procedure for application of the Ca^{2+} fluorescent indicator CaG using high-resolution respirometry (HRR). As some fluorescent dyes affect respiration (Krumschnabel et al 2014; Makrecka-Kuka et al 2015), we evaluated the effect of the probe on respiration. We investigated some limitations caused by common components of respiratory media, to select a medium appropriate for both techniques, and proposed an assay for CaUC determination and a calibration protocol.

2. Materials and methods

2.1. Reagents and media

Calcium Green™-5N, Hexapotassium Salt, cell impermeant (cat. Nº C3737) was obtained from Invitrogen™ (Waltham, USA). From Sigma Aldrich (Burlington, USA): Antimycin A (cat. Nº A8674), ATP (Adenosine 5′-triphosphate disodium salt hydrate, cat. Nº A2383), BSA – fatty acid-free bovine serum albumin (cat. Nº A6003), $CaCl_2$ - calcium chloride 1 M (cat. Nº 21114), CCCP – carbonyl cyanide 3-chlorophenylhydrazone carbonate (cat. Nº C2759), cytochrome *c* (cat. Nº C7752), Na_2EDTA – ethylene diamine tetra acetic acid disodium salt dihydrate (cat. Nº E1644), EGTA– ethylene glycol tetra acetic acid (cat. Nº E4378), glutamate (L-glutamic acid monosodium salt hydrate, cat. Nº G1626), HEPES – 2-[4-(2-hydroxyethyl) piperazin-1-yl]ethanesulfonic acid (cat. Nº H7523), malate (cat. Nº M1000), oligomycin (cat. Nº O4876), KCl – potassium chloride (cat. Nº 60130), KH_2PO_4 – potassium dihydrogen

phosphate (cat. Nº P5655), KOH – potassium hydroxide (cat. Nº P1767), pyruvate (cat. Nº P2256), rotenone (cat. Nº R8875), succinate (cat. Nº S2378), sucrose (cat. Nº S7903) and Tris – Tris-(hydroxymethyl)-aminomethane (cat. Nº 252859). ADP (Adenosine 5'-diphosphate, potassium salt, cat. Nº 117105) was acquired from Millipore (Burlington, USA), $MgCl_2 \cdot 6H_2O$ – magnesium chloride hexahydrate (cat. Nº LC-5041) from Labochem International (Athens, Greece), HCl – hydrochloric acid (cat. Nº 2315957) from Aurelio (Görlitz, Germany). Ethanol 99.9 % (CL0005055000) obtained from Bartelt, Graz, Austria and deionized ultra-pure water (Ultra ClearTM TP UV UF TM) from Evoqua Water Technologies (Pittsburgh, USA) were used to prepare all solutions used.

ADP stock 500 mM with 300 mM $MgCl_2$: 501.3 mg ADP was dissolved in 1.2 mL H_2O; pH was neutralized with 5 M KOH; 122.0 mg $MgCl_2 \cdot 6\ H_2O$ was added, pH was adjusted to 7 at room temperature (RT). ADP 15 mM for calcium uptake measurements was prepared by further dilution with water.

Calcium chloride ($CaCl_2$): 10 mM prepared fresh every experimental day from the 1 M commercial solution, diluted with H_2O.

CaG: 1 mM solution was prepared by dissolving 500 µg of Calcium Green™ in 419 µL H_2O, protected from light and aliquoted for storage.

Cytochrome *c*: 50 mg cytochrome *c* was added to 1 mL H_2O and aliquoted for storage.

EGTA: 20 mM was prepared in H_2O and the pH was adjusted to approximately 7 at RT with KOH to complete dissolution.

Glutamate: 1.691 g glutamate was transferred to a 5 mL volumetric glass flask and dissolved with 4 mL H_2O. After pH adjustment to 7.0 with KOH at RT, the final volume was adjusted to 5 mL (2 M).

Oligomycin: 4 mg oligomycin dissolved in 1 mL ethanol (5 mM) in a glass vial. Aliquots were stored in glass vials.

BIOPS (10 mM Ca^{2+}-EGTA - 0.1 µM free Ca^{2+}, 20 mM imidazole, 20 mM taurine, 50 mM K^+-MES, 0.5 mM dithiothreitol, 6.56 mM $MgCl_2$, 5.77 mM ATP, 15 mM phosphocreatine, pH 7.1 (adjusted with KOH, at 0 °C) was prepared following Fontana-Ayoub et al (2016).

Isolation medium A1: 250 mM sucrose, 0.5 mM Na_2EDTA, 10 mM Tris, pH 7.4, adjusted at 0 °C. prepared following (Fontana-Ayoub et al 2016).

Isolation medium B1: 50 mL Isolation medium A1 and 50 mg BSA prepared fresh on the day of the experiment.

Mitochondrial respiration and calcium medium (MiRCa): 70 mM KCl, 110 mM sucrose, 1 mM $MgCl_2$, 10 mM KH_2PO_4, 20 mM HEPES, pH 7.1 adjusted with KOH 5 M at 30 °C.

MiR05, mitochondrial respiration medium: 0.5 mM EGTA, 3 mM $MgCl_2$, 60 mM lactobionic acid, 20 mM taurine, 10 mM KH_2PO_4, 20 mM HEPES, 110 mM sucrose, 1 $g \cdot L^{-1}$ BSA; pH 7.1; prepared using MiR05-Kit (Oroboros Instruments, Austria, 60101-01) and BSA, pH 7.1 adjusted with KOH 5 M at 30 °C (Baglivio et al 2024).

The other chemicals were prepared as in (Komlodi et al 2021). All solutions and media were aliquoted and stored at -20 °C, unless stated otherwise.

2.2. Animals

Wild-type C57BL/6N adult mice (average age of 15 ± 5 weeks) were housed in the animal facility of Medical University of Innsbruck at a maximum number of five animals per cage. Animals were maintained in a controlled environment (22 °C, 12/12 h light/dark cycle, light period from 7:00 to 19:00) and fed *ad libitum* with free access to water. Mice were killed by cervical dislocation and the liver was immediately removed and placed in ice-cold BIOPS. All procedures were conducted according to the Austrian Animal Experimentation Act in compliance with the European convention for the protection of vertebrate animals used for experimental and other scientific purposes (Tierversuchsgesetz 2012; Directive 2010/63/EU; BMWFM-66.011/0128-WF/V/3b/2016).

2.3. Mitochondrial preparation

Liver mitochondria were isolated following (Lassnig, Gnaiger 2010), with modifications. All steps were performed on ice. Briefly, the wet mass of the whole liver was determined, extensively washed with ice-cold BIOPS, and minced with scissors in Medium A1 with at least three changes of the medium A1 during mincing. The tissue was transferred to a pre-cooled glass/Teflon potter and homogenized in 20 mL of Medium A1 with 5 strokes at ~300 rpm (WiseStir HS-30E, Wisd Laboratory Instruments, Wertheim, Germany), followed by centrifugation at 600 *g* for 10 min at 4 °C (Rotina 380R, Andreas Hettich GmbH & Co. KG, Tuttlingen, Germany). If present, the fluffy white layer was pipetted from the supernatant, which was subsequently centrifuged for 10 min at 10 000 *g* at 4 °C. The supernatant was discarded, and the pellet resuspended with a pipette in 1 mL medium B1, then homogenized with a small glass/Teflon potter in total 5 mL medium B1 with 5 strokes at ~ 300 rpm. More 5 mL B1 was added, and the pellet was centrifuged twice at 10 000 *g* for 10 min at 4 °C and resuspended with a pipette in 10 mL Medium B1 after the 3rd centrifugation and finally, after the 4th centrifugation, it was resuspended in the proportion of 1 g tissue (whole liver wet mass) to 0.5 mL medium B1. The sample was kept on ice for at least 30 min before the experiments. Five µL (only respiratory experiments) or 10 µL (Ca^{2+} experiments) of isolated mitochondria (imt) were added to the 2-mL chambers and the experimental concentration was calculated after protein determination.

Protein concentration was determined using the kit DC Protein Assay (Bio-Rad, Hercules, CA, US), as previously described (Cardoso et al 2021; Komlodi et al 2021).

2.4. High-resolution respirometry and calcium measurements

Ca^{2+} measurements were performed concomitantly with oxygen consumption using the O2k-FluoRespirometer and the software DatLab 7.4 (Oroboros Instruments, Innsbruck, Austria). The measurements were performed at 37 °C in a closed 2-mL glass chamber using black PEEK stoppers and white PVDF stirrer bars. O_2 concentration was measured with polarographic oxygen sensors (POS), and volume-specific O_2 consumption was calculated real-time as the negative time derivative of O_2 concentration. The O_2 flux was corrected by the instrumental O_2 background which was assessed in monthly intervals as part of quality control along with daily air calibration (oxygen sensor test) (Baglivo et al 2022). A polarization voltage of 800 mV was applied to the POS. Data recording interval was set at 2 seconds and stirrer speed at 750 rpm. Respiratory results were expressed as protein-mass specific O_2 flux $J_{V,O2}$ [$pmol \cdot s^{-1} \cdot mg^{-1}$]. Fluorescence was measured with Blue Smart Fluo-Sensors fixed in the front window of the chamber, which have excitation LED 465 nm and filters for LED and photodiode selected for CaG. Fluorescence intensity of 500 and gain 1000 were the amperometric parameters applied and the raw data were obtained in units of nA.

The coupling- and pathway-control protocol SUIT-008 (https://wiki.oroboros.at/index.php/SUIT-008_O2_mt_D026: retrieved 2025-06-16) was applied to compare respiration using MiR05 and MiRCa media in presence or absence of CaG, with the same fluorescence settings as in Ca^{2+} measurements. Rates were determined in the three coupling states, leak respiration *L*, OXPHOS capacity *P*, and electron transfer (ET) capacity *E*. After addition of imt (residual endogenous substrates *ren*), 5 mM pyruvate and 2 mM malate (PM) were added as a combination of substrates for the NADH-linked pathway (N_L). This was followed by addition of 2.5 mM ADP (D; N_P), then 10 µM cytochrome *c* (*c*; Nc_P), 10 mM glutamate (G; N_P), 10 mM succinate (S; NS_P). The uncoupler CCCP was titrated in multiple steps (U; 0.5 – 3.5 µM) until maximum respiration (NS_E) was achieved. Then, 0.5 µM rotenone (Rot; S_E), and 2.5 µM antimycin A (Ama; *rox*) were added sequentially. All mitochondrial respiratory rates were baseline-corrected for residual oxygen consumption (*rox*).

CaG, hexapotassium salt does not cross cellular membranes, therefore the extramitochondrial Ca^{2+} was measured. The SUIT-035_mt_CaG_D083 protocol was applied for concomitant Ca^{2+} and oxygen measurement in liver imt using MiRCa as respiration medium. Addition of CaG 2 µM was followed by glutamate 10 mM and malate 2 mM as NADH-linked substrates. Then ADP was added at a low concentration (30 µM), which is needed to achieve consistent Ca^{2+} uptake, inhibiting possibly already assembled mtPTP (Saito, Castilho 2010), and is in the physiological cytosolic concentration for cellular resting states (Rottenberg, Marbach 1990; Williams et al 1993). To ensure a high mtMP, oligomycin (Omy, 2.5 µM) was added to induce the leak state required for Ca^{2+} uptake. EGTA 15 µM was added to chelate the Ca^{2+} contamination of the medium and chemicals, followed by addition of imt (~0.1 $mg \cdot mL^{-1}$), and $CaCl_2$ (Ca^{2+}) was titrated in 5 µM steps. Finally, uncoupler was titrated after mtPTP opening to ensure that all Ca^{2+} was released. Glutamate increased the

background fluorescence signal, while malate decreased it. Taken together, no correction had to be applied.

In initial experiments, EGTA was titrated in 5 µM steps until no further decrease in the CaG signal was observed. In subsequent experiments, a single EGTA step of 15 µM was used. The EGTA concentration must be evaluated for every sample type and medium batch, as some chemicals used to prepare media can contain low Ca^{2+} concentrations, which should be chelated before titrating the sample. If the EGTA concentration is too high, the CaG signal does not respond to $CaCl_2$ titrations, indicating a lack of Ca^{2+} uptake. Conversely, if [EGTA] is too low, contaminant Ca^{2+} in the medium may be taken up by mitochondria before the titrations. The latter can be observed as a decrease in the CaG signal after adding mitochondria, similar to what is observed during Ca^{2+} uptake, instead of a rapid decrease and subsequent stabilization of the signal. Hence, for the first experiment with a new sample type, EGTA should be titrated stepwise before addition of mitochondria, until the decrease in the CaG signal is minimal.

$CaCl_2$ titration steps should be optimized based on sample concentration and tissue type, as mitochondrial permeability transition (mtPT) induction thresholds vary with tissue origin and potential sensitizing factors (Vercesi et al 2018). Our preliminary tests compared 2.5 µM and 5 µM Ca^{2+} steps.

The Titration-Injection microPump (TIP2k, Oroboros Instruments, Innsbruck, Austria) was used for some measurements. The syringes were filled with 10 mM $CaCl_2$ following the manufacturer's instructions (Gradl et al 2021). The TIP2k was programmed to titrate 0.5 or 1 µL of $CaCl_2$ (2.5 and 5 µM experimental concentration, respectively) during one second every 5 or 6 minutes. In continuous Ca^{2+} injection experiments the TIP2k was set to inject 10 nM of Ca^{2+} per second (2 $nL \cdot s^{-1}$). At such a low volume injection rate the amount of O_2 added into the chamber with the $CaCl_2$ solution is negligible and corrections are not required (Gnaiger 2001). The titrations were stopped manually after Ca^{2+} release was observed.

Ca^{2+} calibration curves were obtained under experimental conditions, in the absence or presence of mitochondria when Ca^{2+} uptake was inhibited. We used the MCU inhibitor ruthenium red (RR, 1 µM) or inhibited the mitochondria electron transfer system and collapsing the protonmotive force with an inhibitor cocktail containing rotenone and antimycin A, and the uncoupler CCCP (Rot, 0.5 µM; Ama, 2.5 µM; and CCCP, 1 µM). The TIP2k was programmed to inject 1 µL of $CaCl_2$ in one second every 2 minutes, to a total of 10 titrations of 5 µM $CaCl_2$. To calculate the extramitochondrial Ca^{2+} concentration [Ca^{2+}], the CaG raw signals (I, nA) obtained during sections (setting marks in DatLab) after each $CaCl_2$ titration with known concentration were fitted by a second-degree polynomial (Eq. 1).

$$[Ca^{2+}] = aI^2 + bI + c \qquad \text{Eq. 1}$$

Independent experiments were repeated five to eight times, with different mitochondrial preparations.

2.5. Data analysis

Data analysis of O_2 measurements in SUIT-008 was performed using Excel templates provided with DatLab 7.4 and statistical analyses were performed with GraphPad Prism 9 or 10 software.

3. Results and discussion

3.1. The medium MiRCa and the fluorophore CaG do not affect respiration

Finding a medium that suits both Ca^{2+} uptake analysis and respiration was a major challenge. The most suited medium for respiration, MiR05, cannot be used to analyze Ca^{2+} uptake due to many components that interfere with the Ca^{2+} signal, such as high concentration of EGTA, and the presence of lactobionic acid, taurine and BSA (Nászai et al 2019). On the other hand, media used for Ca^{2+} uptake measurements frequently contain low phosphate concentration and high KCl concentration, which decrease respiratory rates (Wollenman et al 2017; Doerrier et al 2024). Mitochondrial Respiration and Calcium medium MiRCa, containing a low KCl concentration and the same phosphate concentration as MiR05 was developed to measure simultaneously respiration and CaG signal. MiRCa and MiR05 had identical mass-specific mitochondrial O_2 flux (*rox* corrected) supported by pyruvate, malate, and glutamate (N-pathway), plus succinate (NS-pathway) in different coupling states, and the S-pathway after inhibition by rotenone (Table S1, *p*-values comparing media effect).

The fluorescent dyes safranin, rhodamine and Amplex Red used to evaluate mitochondrial function, such as mtMP and hydrogen peroxide production, can alter mitochondrial respiration (Scaduto, Grotyohann 1999; Krumschnabel et al 2014; Makrecka-Kuka et al 2015). In contrast, Magnesium Green (MgG), used to measure ATP production did not affect respiration (Cardoso et al 2021). Similarly, there was no effect of CaG on mitochondrial O_2 flux (Figure 1a; $p > 0.3$), as highlighted by expressing respiration in the presence of CaG relative to the control (Figure 1b).

Flux control ratios (*FCR*) are statistically more robust to evaluate differences in mitochondrial respiratory control patterns. *FCR* were not different in MiRCa and MiR05 (Figure 1c), except for a possible trend of MiRCa for a lower S_E/NS_E ratio (6Rot in Table S2), and N_P/NS_E in the presence of CaG (2D and 2c in Table S2; comparison of the presence to the absence of CaG in *FCR* generate $p > 0.3$). When combining groups with and without CaG, lower *p*-values were observed in NS_P and S_E in both protein mass-specific O_2 flux and *FCR* (Tables S3 and S4). Figure 1d shows the relative media effect. These results indicate that comparable to MgG, CaG does not affect respiration, and MiRCa is a suitable medium for combined respiration and calcium measurements using CaG.

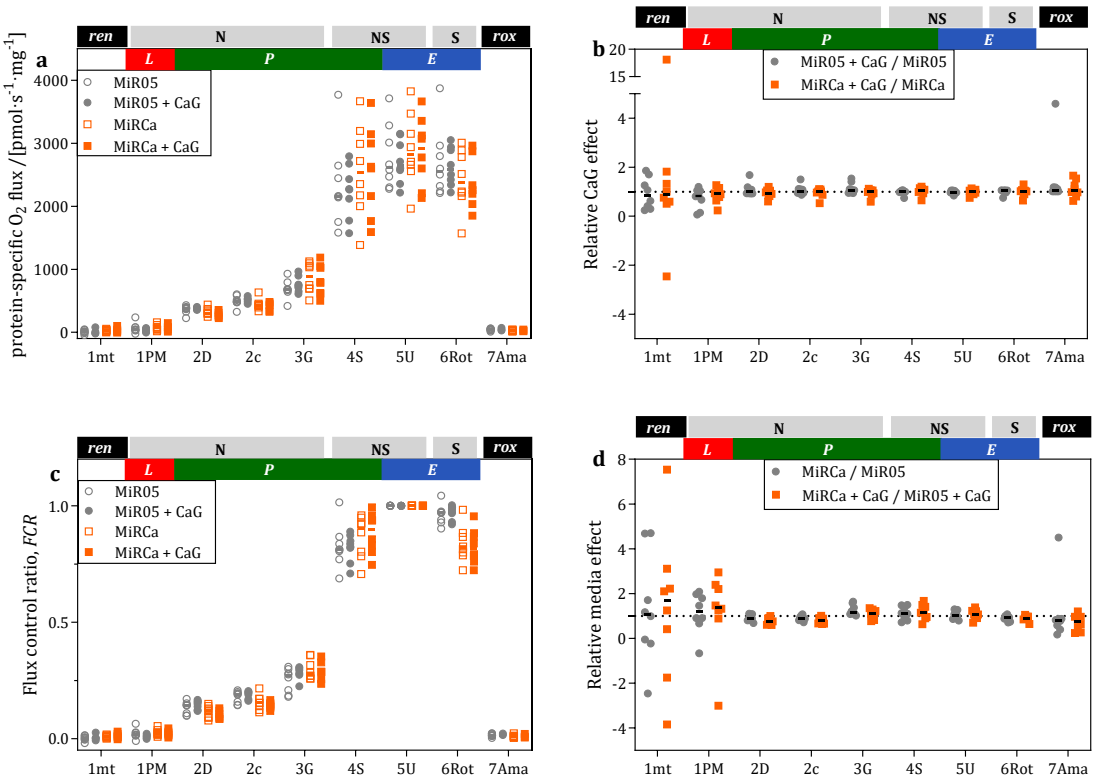

Figure 1: The effect of CaG on O_2 consumption of mitochondria isolated from mouse liver in MiR05 and MiRCa media. HRR with coupling control protocol SUIT-008_O2_mt_D026, before addition of substrates (*ren*), N-, NS-, and S-linked pathways in different coupling states, and finally *rox* after inhibition by Ama. The sequential titrations are indicated on the abscissas. Different symbols and colors indicate the treatments, each symbol represents an independent mitochondrial preparation, and for every preparation, all treatments were tested in parallel at the same time. 7Ama not *rox*-corrected. **(a)** mitochondrial protein-specific flux, *rox*-corrected, **(b)** Relative CaG effect calculated by dividing O_2 fluxes measured in the presence by those in the absence of CaG. **(c)** *FCR* *rox*-corrected. Lines represent the medians. **(d)** Relative media effect calculated by dividing O_2 fluxes measured with MiRCa by those measured with MiR05, in the presence or absence of CaG. Sample protein concentration 0.0515 ± 0.0068 mg · mL^{-1} (median ± standard deviation, SD).

3.2. Calcium uptake

Representative traces show simultaneously monitored mitochondrial respiration (Figure 2a and 3a) and the CaG signal in a sequence of Ca^{2+} titrations (Figure 2b and 3b). Glutamate & malate were used as substrates in the leak state. Since CaG is membrane impermeable, the fluorescence signal is a function of the Ca^{2+} concentration in the incubation medium outside the mitochondria.

The response of the Ca^{2+} signal was small and no Ca^{2+} uptake was indicated after the first or even second Ca^{2+} titrations of 2.5 µM (Figure 2) or 5 µM (Figure 3), most probably due to binding by the initially added EGTA (15 µM). An increased

response of the Ca^{2+} signal indicates EGTA chelation in the initial titration steps, while an identical increase indicates that EGTA chelation is saturated. There was no Ca^{2+} uptake, up to a total addition of 5 µM (second titration of 2.5 µM or first titration of 5 µM). This reflects the high apparent K_d of the MCU, requiring elevated Ca^{2+} levels (Giorgi et al 2018). Upon two or more additional Ca^{2+} titrations, Ca^{2+} uptake was complete in each step, as indicated by the decline of the Ca^{2+} signal to the level obtained before the titration (Figure 2b and 3b). An increase of the Ca^{2+} signal beyond the titrated concentration indicated mtPT. Towards mtPT, Ca^{2+} uptake was incomplete, i.e., less than the 2.5 or 5 µM titrated. CsA delayed mtPT (Figure 2b and 3b, green line).

O_2 flux increased transiently during episodes of Ca^{2+} uptake after 5 µM Ca^{2+} titrations and returned to pre-titration levels when the rate of Ca^{2+} uptake levelled off (Figure 3a). The respiratory response to 2.5 µM titrations was too low to be resolved from noise. mtPTP opening led to sharp inhibition of respiration which subsequently could not be stimulated by the uncoupler CCCP.

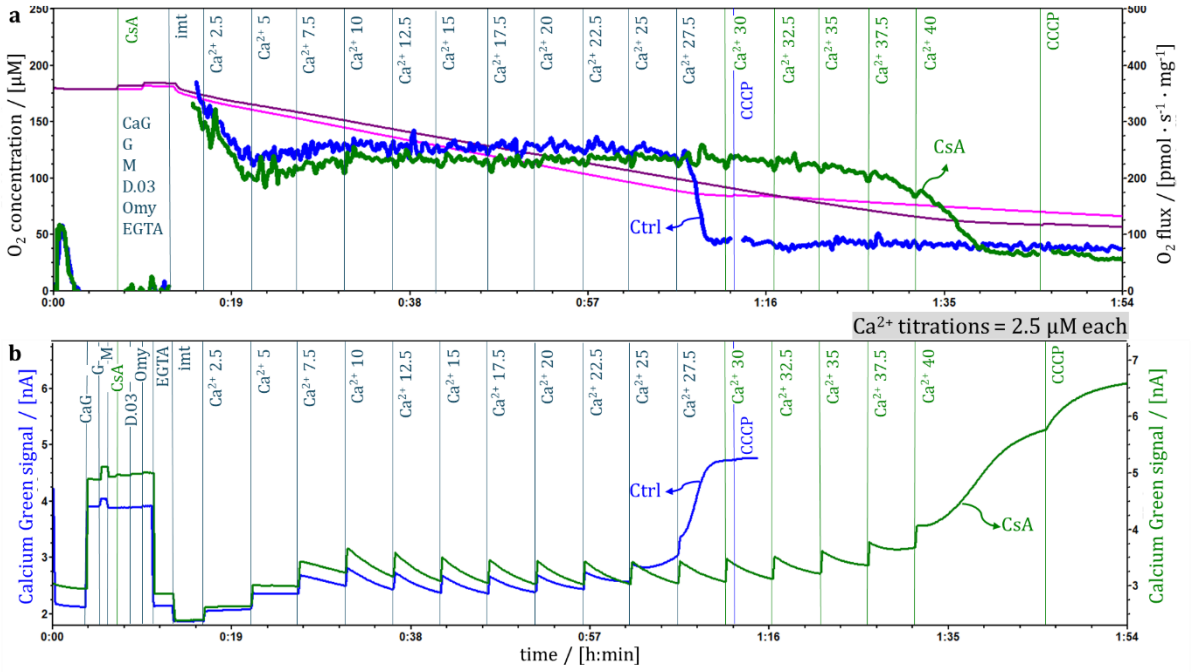

Figure 2: Respiration and calcium uptake with 2.5 µM Ca^{2+} titration steps. Representative traces (protocol SUIT-035_CaG_D083) with glutamate (G, 10 mM) and malate (M, 2 mM) as substrates in the leak(Omy) state. Cyclosporin A (CsA, 1 µM), Calcium Green (CaG, 2 µM), ADP (30 µM), Oligomycin (Omy, 20 nM), and EGTA added before isolated mitochondria (imt). Subsequently, $CaCl_2$ was titrated in 2.5 µM steps (Ca^{2+}) every 5 min until calcium release was observed as an increase in the CaG signal. Dark blue vertical lines represent events in both chambers, blue in chamber A and green in chamber B. **(a)** O_2 concentration (pink and purple lines), specific O_2 flux in the absence (blue line, Ctrl) or presence of CsA (green line, CsA). **(b)** CaG signal in the absence (blue line, Ctrl) or presence of CsA (green line, CsA). Experiment 2021-02-17 P7-02.

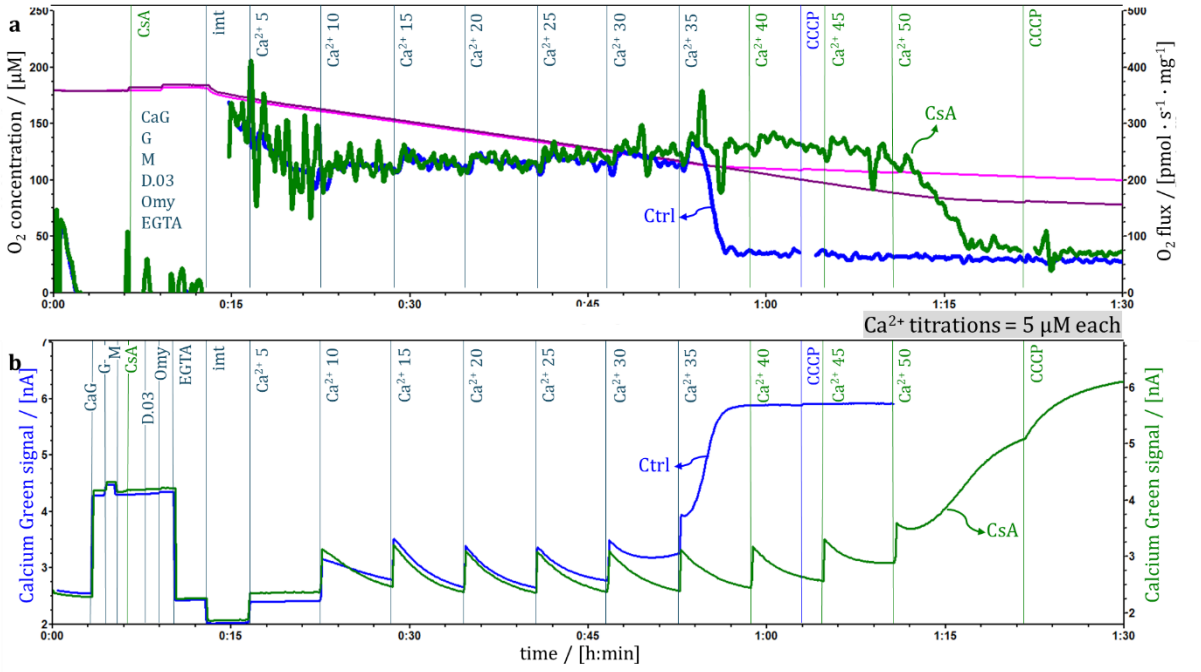

Figure 3: Respiration and calcium uptake with 5 µM Ca^{2+} titration steps. Representative traces (protocol SUIT-035_CaG_D083) with glutamate (G, 10 mM) and malate (M, 2 mM) as substrates in the leak(Omy) state. Cyclosporin A (CsA, 1 µM), Calcium Green (CaG, 2 µM), ADP (30 µM), Oligomycin (Omy, 20 nM), and EGTA added before isolated mitochondria (imt). Subsequently, $CaCl_2$ was titrated in 5 µM steps (Ca^{2+}) every 5 min until calcium release was observed as an increase in the CaG signal. Dark blue vertical lines represent events in both chambers, blue in chamber A and green in chamber B. **(a)** O_2 concentration (pink and purple lines), specific O_2 flux in the absence (blue line, Ctrl) or presence of CsA (green line, CsA). **(b)** CaG signal in the absence (blue line, Ctrl) or presence of CsA (green line, CsA). Experiment 2021-02-17 P8-02.

In preliminary experiments, in controls with 2.5 µM Ca^{2+} titrations the mtPT was triggered after 25 µM Ca^{2+} added (26.6 µM ± 1.2, mean ± standard deviation, SD, N = 3), while by adding Ca^{2+} in 5 µM steps, the mtPT was triggered after 30 µM Ca^{2+} (31.6 µM ± 2.4, mean ± SD, N = 3). Lower concentrations could underestimate the total Ca^{2+} uptake which is probably related to the time of exposure of mitochondria to Ca^{2+} (Drahota et al 2020). Conversely, larger Ca^{2+} pulses may exceed physiological concentrations, such as those seen in ER/SR Ca^{2+} release waves (Csordás et al 1999; Rizzuto et al 2012).

Figure 4 shows representative traces of mitochondrial respiration and CaG signal upon continuous injection of Ca^{2+} with the TIP2k at 10 nM/s, with the same substrates mentioned previously. Initially, the CaG signal increased up to 12.3 µM ± 1.4, (mean ± SD, N = 3) until the capacity for EGTA chelation and a concentration sufficient for kinetic control of the low-affinity MCU were reached. A near steady-state was reached where the net-uptake rate overcompensates slightly the Ca^{2+} injection rate. Afterwards, the CaG signal increased steeply, indicating mtPT. The oxygen flux in response to continuous injections was similar to that in experiments with 2.5 µM Ca^{2+} step titrations.

The different approaches of Ca^{2+} titrations (single bolus, pulses with different concentrations or injections) leads to different Ca^{2+} additions necessary to trigger mtPT, as observed previously (Chalmers, Nicholls 2003). In that study the authors observed that the capacity of rat liver mitochondria to accumulate Ca^{2+} before mtPT was 800 nmol·mg^{-1} using a steady infusion, compared to 650 nmol·mg^{-1} using pulses, or 450 nmol·mg^{-1} in a single bolus.

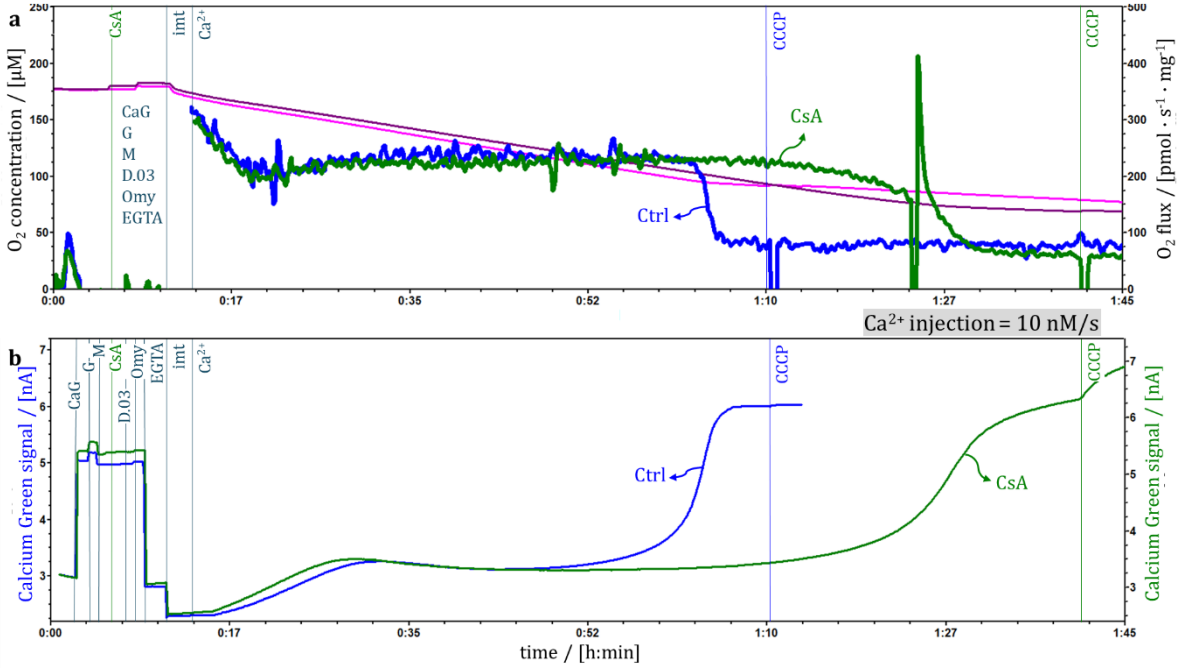

Figure 4: Respiration and calcium with continuous injection of Ca^{2+}. Representative traces of the calcium injection protocol with glutamate (G, 10 mM) and malate (M, 2 mM) as substrates in the leak(Omy) state. Cyclosporin A (CsA, 1 µM), Calcium Green (CaG, 2 µM), ADP (30 µM), Oligomycin (Omy, 20 nM), and EGTA were added before isolated mitochondria (imt). Subsequently, $CaCl_2$ was injected by the TIP2k at a rate of 10 nM/s (Ca^{2+}) until calcium release was observed as an increase in the CaG signal. Dark blue vertical lines represent events in both chambers, blue in chamber A and green in chamber B. **(a)** O_2 concentration (pink and purple lines), specific O_2 flux in the absence (blue line, Ctrl) or presence of CsA (green line, CsA). **(b)** CaG signal in the absence (blue line, Ctrl) or presence of CsA (green line, CsA). Experiment 2021-02-17 P5-02.

3.3. Calibrations of Calcium Green signal

Ca^{2+} additions required to trigger mtPT can be calculated either from the non-calibrated CaG signal or from the O_2 flux, which is frequently defined as CaRC (Basso et al 2008; Doczi et al 2016; Li et al 2018; Harisseh et al 2019; Deak et al 2021; Ghazal, Kwong 2025). To obtain the actual Ca^{2+} concentration in solution, the Ca^{2+} signal has to be calibrated taking into account the non-linearity of fluorescence methods (Chinopoulos et al 2014). Without standardized calibration, reproducibility between studies is compromised, preventing a coherent understanding of Ca^{2+}-dependent processes.

Using a spectrofluorometer, it is possible to obtain calibrations which consider the K_d (Amigo et al 2017; Duong et al 2020), maximal and minimal fluorescence, applied to (Eq. 2),

$$[Ca^{2+}] = K_d \cdot \frac{(F - F_{min})}{(F_{max} - F)} \quad \text{Eq. 2}$$

In the present experimental conditions used to measure Ca^{2+} (CaG concentration and fluo intensity) and gain setting, the high Ca^{2+} concentration required to obtain F_{max} would saturate the amplifier at a maximum of 10 µA. Lower CaG concentration, gain and fluo intensity could counteract this limitation, but the sensitivity and the signal resolution to evaluate the Ca^{2+} titration steps would be reduced. One possibility is to inhibit Ca^{2+} uptake of mitochondria and titrate Ca^{2+} to get a standard calibration curve (see supplementary material). Ruthenium red RR is frequently used as a MCU inhibitor, preventing Ca^{2+} uptake. A disadvantage of using RR in the Oroboros platform is a carry-over of an inhibitory effect to subsequent experiments. Alternatively, Ca^{2+} uptake can be inhibited by an inhibitor cocktail containing rotenone, antimycin A and the uncoupler CCCP.

3.4. Applying the calibration

In the Ca^{2+} uptake experiments performed with several Ca^{2+} titrations (Figure 3), marks were set for each step at the highest CaG signal and subsequently at the lowest signal before the next 5 µM Ca^{2+} titration, representing the addition of Ca^{2+} and Ca^{2+} uptake, respectively. After the experiment with the same sample and RR or inhibitor cocktail, a calibration was performed, creating a polynomial second-order function. The fluorescence raw values (nA) of the marks from the Ca^{2+} uptake experiments were applied for polynomial fitting.

Figure 5 shows the calculated concentration differences ΔCa^{2+} in response to Ca^{2+} titrations. Unexpectedly, from the third titration onwards, the majority of calculated ΔCa^{2+} concentrations were higher than the 5 µM step. Theoretically, lower values than the 5 µM steps might be expected due to rapid Ca^{2+} uptake or chelation by medium components. The fluorescence signal before the first Ca^{2+} titration were similar in experiments with functional mitochondria and calibrations with inhibited mitochondria and cannot explain the observed differences. We currently lack a mechanistic explanation for the >5 µM Ca^{2+} concentration response. In conclusion, the polynomial calibration method is unreliable under these experimental conditions. Therefore, we developed an intra-experimental calibration approach.

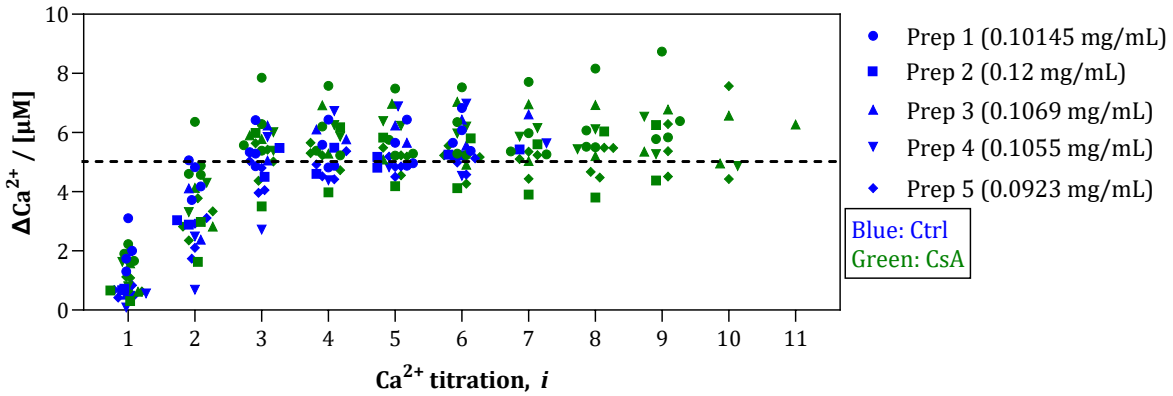

Figure 5. Calcium concentration of 5 µM Ca^{2+} titrations during calcium uptake measurements assessed by polynomial fit calibration. Calibration curves were obtained for each sample and combination of Fluo-Sensor and O2k immediately after the calcium uptake measurements. Different symbols indicate independent sample preparations, every symbol indicates technical repeats, blue symbols represent Ctrl and green symbols CsA.

To convert changes in fluorescence to changes in Ca^{2+} concentration, the sequential 5 µM Ca^{2+} titrations, $\Delta c_{in(i)}$ (Figure 6a and b), were divided by the corresponding step changes in fluorescence signal ΔFS_i, where i indicates sequential titrations. These yield corresponding calibration factors f_i (Eq. 3),

$$f_i = \frac{\Delta c_{in(i)}}{\Delta FS_i} \quad [\mu M/\mu A] \qquad \text{Eq. 3}$$

ΔFS_i and hence f_i changed as a nonlinear function of the titration steps i (Figure 6c to e). Therefore, the following equation was used to calculate average calibration factors $f_{calc(i)}$,

$$f_{calc(i)} = \frac{\Delta c_{in(i)}}{\Delta FS_{calc(i)}} \quad [\mu M/\mu A] \qquad \text{Eq. 4}$$

where $\Delta FS_{calc(i)}$ is

for $r_{u(i)} < 1$ $$\Delta FS_{calc(i)} = \frac{(1+r_{u(i)})\cdot\Delta FS_i + (1-r_{u(i)})\cdot\Delta FS_{i+1}}{2} \quad [\mu A] \qquad \text{Eq. 5a}$$

for $r_{u(i)} > 1$ $$\Delta FS_{calc(i)} = \frac{(1+r_{u(i)})\cdot\Delta FS_{i-1} + (1-r_{u(i)})\cdot\Delta FS_i}{2} \quad [\mu A] \qquad \text{Eq. 5b}$$

and the Ca^{2+} uptake ratio $r_{u(i)}$

$$r_{u(i)} = \frac{\Delta FS_{u(i)}}{\Delta FS_i} \qquad \text{Eq. 6}$$

When the $r_{u(i)}$ is <1, the uptake was incomplete and $\Delta FS_{calc(i)}$ was calculated from ΔFS_i and ΔFS_{i+1}, the step changes in fluorescence before and after the Ca^{2+} uptake (Figure 6b, i = 3). When the $r_{u(i)}$ was >1, the uptake was higher than the $\Delta c_{in(i)}$ and $\Delta FS_{calc(i)}$ was calculated from ΔFS_{i-1} and ΔFS_i by interpolation (Figure 6b, i = 4).

Ca^{2+} uptake $\Delta c_{u(i)}$ was calculated as the decrease in the fluorometric signal $\Delta FS_{u(i)}$ multiplied by the calibration factor $f_{calc(i)}$,

$$\Delta c_{\mathrm{u}(i)} = f_{\mathrm{calc}(i)} \cdot \Delta FS_{\mathrm{u}(i)} \quad [\mu M] \qquad \text{Eq. 7}$$

n is the titration step *i* when the fluorescence signal increased due to mtPT. The calcium uptake capacity (CaUC; Figure 6b) is calculated as,

$$\mathrm{CaUC} = \sum_{i=1}^{n} (\Delta c_{\mathrm{u}(i)})_n \ [\mu M] \qquad \text{Eq. 8}$$

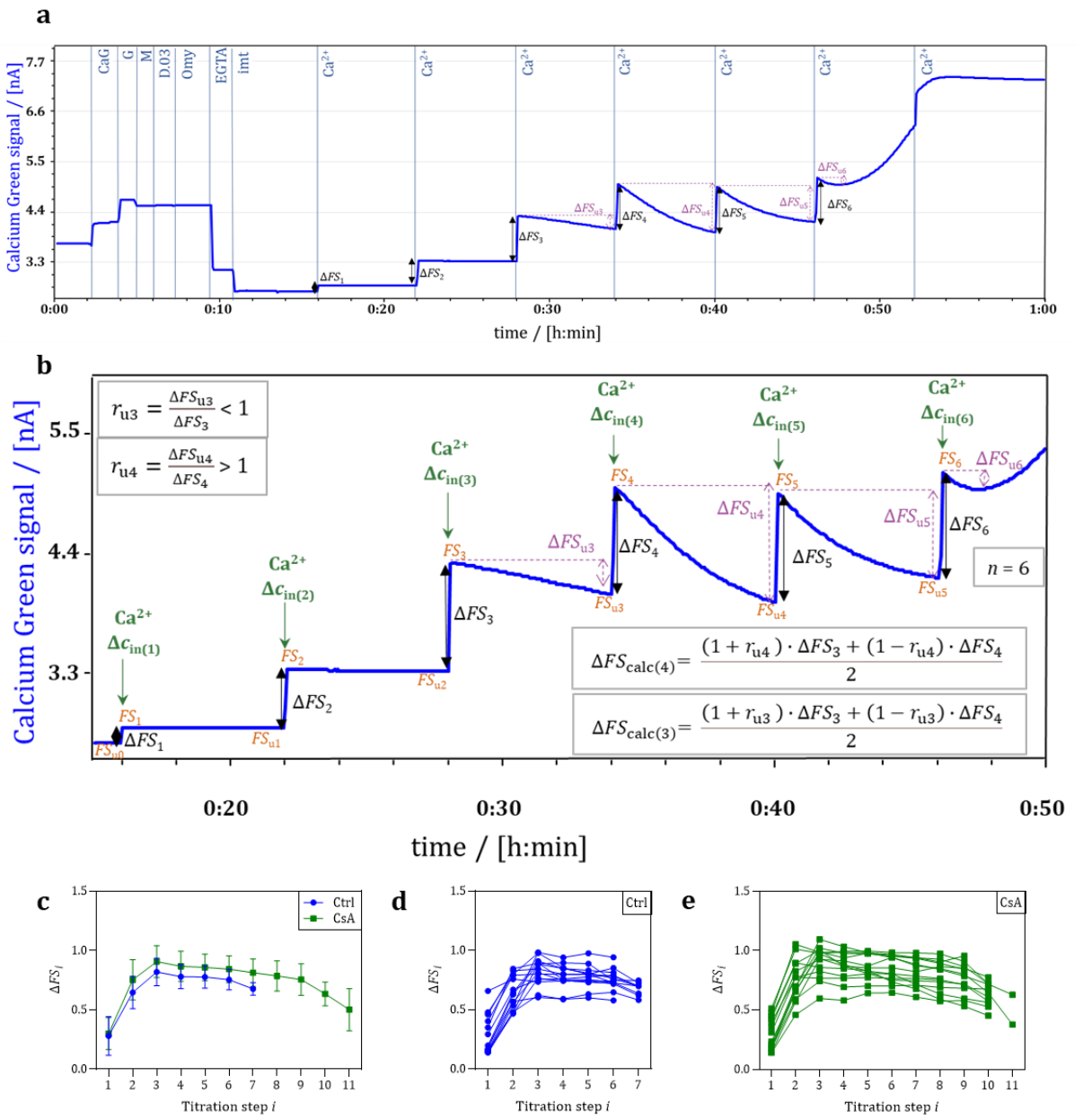

Figure 6: Intraexperimental calibration of calcium signal. ΔFS_i is the difference of the peak fluorescence signal measured after a 5 µM Ca^{2+} pulse (Δc_{in}) and the *FS* immediately before. ΔFS_{iu} is the difference of the peak FS_{i-1} and the *FS* immediately before the next Ca^{2+} titration. **(a)** Representative trace indicating ΔFS_i and ΔFS_{iu} used in Eq. 3-8. Black arrows indicate ΔFS_i and blue dashed arrows indicate ΔFS_{iu}. All ΔFS_{iu} were added to provide corrected CaUC. Experiment 2021-09-02 P3-02. **(b)** Zoom from panel (a). Green arrows represent 5 µM Ca^{2+} titrations, Δc_{in}. $\Delta FS_{calc(i)}$ calculation (equations shown) changes if uptake was higher than

respectively ΔFS_i (r>1) or if the uptake was incomplete (r<1). **(c), (d)** and **(e)** show ΔFS for each ΔCa^{2+} concentration from all experiments. Red lines represent the experiments in absence of CsA, Ctrl and green lines in presence of CsA. Mean ± SD in **(c)** and each replicate in **(d)** and **(e)**. See Table 1 for definition of abbreviations.

Table 1: Abbreviations from Equations 3-8 and Figure 6.

abbreviation	meaning
$f_{calc(i)}$	calibration factors calculated
f_i	calibration factors
i	sequential titrations, single step
n	number of the step in which mtPT occurs
$r_{u(i)}$	Ca^{2+} uptake ratio
$\Delta c_{in(i)}$	variation of concentration due to sequential 5 µM Ca^{2+} titrations
$\Delta c_{u(i)}$	variation of concentration due to Ca^{2+} uptake
$\Delta FS_{calc(i)}$	step changes in fluorescence signal calculated
ΔFS_i	step changes in fluorescence signal
ΔFS_{i+1}	changes in fluorescence signal in the next step
ΔFS_{i-1}	changes in fluorescence signal in the previous step
$\Delta FS_{u(i)}$	decrease in the fluorescence signal

The advantage of applying the polynomial fit equation is that it is a very widespread procedure, but for the CaG signal under the present experimental conditions it yields Ca^{2+} concentrations higher than expected from the titrations. The intraexperimental calibration counteracts this and, importantly, does not require a second experimental run.

While the present method offers significant advantages for simultaneous monitoring of calcium dynamics and mitochondrial respiration, it also has limitations. Specifically, using isolated mitochondria, although advantageous for experimental control, may not fully recapitulate the complexity of intact cells or tissues. Furthermore, the use of CaG restricts its application to mitochondrial preparations since the dye does not effectively permeate the plasma membrane. Consequently, this approach cannot be directly extended to living cells or intact tissues, where calcium signaling is regulated by additional compartments and mechanisms. Using permeabilized cells and permeabilized tissues which better preserve the structural and regulatory context of mitochondria compared to isolated organelles, could broaden the physiological relevance while maintaining control over the experimental environment.

Future studies could apply this method to assess tissue-specific differences in mitochondrial calcium handling, or to investigate disease models characterized by altered calcium homeostasis.

Importantly, our intra-experiment calibration strategy improves reproducibility by eliminating possible confounding factors due to interactions between CaG and inhibited mitochondria. Moreover, by providing a standardized method to quantify calcium uptake capacity, this technique can help reduce the variability between

laboratories (Endlicher et al 2023), improving the reproducibility and comparability of mitochondrial calcium handling studies.

4. Conclusions

Accurate quantification of mitochondrial Ca^{2+} uptake is essential for understanding its dual role in cellular metabolism and death signaling; however, the lack of standardized experimental methods across laboratories hampers reproducibility and limits meaningful data comparison. Establishing quality-controlled protocols is critical to advance both basic research and therapeutic development in Ca^{2+}-mediated mitochondrial function.

The calibration method presented in this study enables accurate quantification of Ca^{2+} uptake by mitochondria without the need for external calibration procedures, thereby reducing sample requirements and streamlining experimental workflow. Using a medium developed for Ca^{2+} measurements without negative impact on respiratory capacities ensures that experimental conditions do not interfere with mitochondrial function.

This approach facilitates a more integrated analysis of mitochondrial calcium handling and respiration. In fact, using the Oroboros, many more techniques can be combined and measured simultaneously in two different chambers.

The broader applicability of this method of calcium calibration will be presented in a different study on the topic of calcium retention capacity.

Abbreviations

CaG	Calcium Green
CaRC	calcium retention capacity
CaUC	calcium uptake capacity
CsA	Cyclosporin A
ER	endoplasmic reticulum
FCR	flux control ratio
HRR	high-resolution respirometry
imt	isolated mitochondria
MgG	Magnesium Green
mtIM	mitochondrial inner membrane
MCU	mitochondrial calcium uniporter
mtMP	mitochondrial membrane potential
mtPT	mitochondrial permeability transition
mtPTP	mitochondrial permeability transition pore
MiRCa	mitochondrial respiration and calcium medium
MiR05	mitochondrial respiratiom medium
POS	polarographic oxygen sensor
RR	ruthenium red
SR	sarcoplasmic reticulum
SD	standard deviation
TIP2k	Titration-Injection microPump
VDAC	voltage-dependent anion channel

Acknowledgements

This work was supported by project NextGen-O2k which has received funding from the European Union's Horizon 2020 research and innovation programme under grant agreement Nº 859770.

References

Ahn B, Ranjit R, Kneis P, Xu H, Piekarz KM, Freeman WM, Kinter M, Richardson A, Ran Q, Brooks SV, Van Remmen H (2022) Scavenging mitochondrial hydrogen peroxide by peroxiredoxin 3 overexpression attenuates contractile dysfunction and muscle atrophy in a murine model of accelerated sarcopenia. https://doi.org/10.1111/acel.13569

Amigo I, Menezes-Filho SL, Luévano-Martínez LA, Chausse B, Kowaltowski A (2017) Caloric restriction increases brain mitochondrial calcium retention capacity and protects against excitotoxicity. https://doi.org/10.1111/acel.12527

Baglivo E, Cardoso LHD, Cecatto C, Gnaiger E (2022) Statistical analysis of instrumental reproducibility as internal quality control in high-resolution respirometry. https://doi.org/10.26124/bec:2022-0008

Baglivo E, Cardoso LHD, Cecatto C, Gnaiger E (2024) Stability of mitochondrial respiration medium used in high-resolution respirometry with living and permeabilized cells. https://doi.org/10.26124/bec.2024-0008

Balaban RS (2009) The role of Ca^{2+} signaling in the coordination of mitochondrial ATP production with cardiac work. https://doi.org/10.1016/j.bbabio.2009.05.011

Basso E, Petronilli V, Forte MA, Bernardi P (2008) Phosphate is essential for inhibition of the mitochondrial permeability transition pore by cyclosporin A and by cyclophilin D ablation. https://doi.org/10.1074/jbc.C800132200

Bernardi P, Rasola A, Forte M, Lippe G (2015) The mitochondrial permeability transition pore: Channel formation by F-ATP synthase, integration in signal transduction, and role in pathophysiology. https://doi.org/10.1152/physrev.00001.2015

Bernardi P, Gerle C, Halestrap AP, Jonas EA, Karch J, Mnatsakanyan N, Pavlov E, Sheu SS, Soukas AA (2023) Identity, structure, and function of the mitochondrial permeability transition pore: controversies, consensus, recent advances, and future directions. https://doi.org/10.1038/s41418-023-01187-0

Berridge MJ, Lipp P, Bootman MD (2000) The versatility and universality of calcium signalling. https://doi.org/10.1038/35036035

Cardoso LHD, Doerrier C, Gnaiger E (2021) Magnesium Green for fluorometric measurement of ATP production does not interfere with mitochondrial respiration. https://doi:10.26124/bec:2021-0001

Carraro M, Bernardi P (2023) The mitochondrial permeability transition pore in Ca^{2+} homeostasis. https://doi.org/10.1016/j.ceca.2023.102719

Carvalho EJ, Stathopulos PB, Madesh M (2020) Regulation of Ca^{2+} exchanges and signaling in mitochondria. https://doi.org/10.1016/j.cophys.2020.08.010

Chalmers S, Nicholls DG (2003) The relationship between free and total calcium concentrations in the matrix of liver and brain mitochondria. https://doi.org/10.1074/jbc.M212661200

Chinopoulos C, Kiss G, Kawamata H, Starkov AA (2014) Measurement of ADP-ATP exchange in relation to mitochondrial transmembrane potential and oxygen consumption. https://doi.org/10.1016/B978-0-12-416618-9.00017-0

Clapham DE (2007) Calcium signaling. https://doi.org/10.1016/j.cell.2007.11.028

Csordás G, Thomas AP, Hajnóczky G (1999) Quasi-synaptic calcium signal transmission between endoplasmic reticulum and mitochondria. https://doi.org/10.1093/emboj/18.1.96

De Mario A, D'Angelo D, Zanotti G, Raffaello A, Mammucari C (2023) The mitochondrial calcium uniporter complex-A play in five acts. https://doi.org/10.1016/j.ceca.2023.102720

Deak AT, Jean-Quartier C, Bondarenko AI, Groschner LN, Malli R, Graier WF, Waldeck-Weiermair M (2021) Assessment of Mitochondrial Ca^{2+} Uptake. https://doi.org/10.1007/978-1-0716-1266-8_13

Deline ML, Grashei M, van Heijster FHA, Schilling F, Straub J, Fromme T (2021) Adenylate kinase derived ATP shapes respiration and calcium storage of isolated mitochondria.

https://doi.org/10.1016/j.bbabio.2021.148409
Denton RM (2009) Regulation of mitochondrial dehydrogenases by calcium ions. https://doi.org/10.1016/j.bbabio.2009.01.005
Doczi J, Torocsik B, Echaniz-Laguna A, De Camaret BM, Starkov A, Starkova N, Gál A, Molnár MJ, Kawamata H, Manfredi G, Adam-Vizi V, Chinopoulos C (2016) Alterations in voltage-sensing of the mitochondrial permeability transition pore in ANT1-deficient cells. https://doi.org/10.1038/srep26700
Doerrier C et al (2024) Harmonization of experimental procedures to assess mitochondrial respiration in human permeabilized skeletal muscle fibers. https://doi.org/10.1016/j.freeradbiomed.2024.07.039
Donnelly C et al (2024) Functional hypoxia reduces mitochondrial calcium uptake. https://doi.org/10.1016/j.redox.2024.103037
Drahota Z, Endlicher R, Kučera O, Rychtrmoc D, Červinková Z (2020) Factors affecting the function of the mitochondrial membrane permeability transition pore and their role in evaluation of calcium retention capacity values. https://doi.org/10.33549/PHYSIOLRES.934391
Duchen MR (2004) Roles of mitochondria in health and disease. https://doi.org/10.2337/diabetes.53.2007.S96
Duong QV, Hoffman A, Zhong K, Dessinger MJ, Zhang Y, Bazil JN. (2020) Calcium overload decreases net free radical emission in cardiac mitochondria. https://doi.org/10.1016/j.mito.2020.01.005
Duvvuri B, Lood C (2021) Mitochondrial Calcification. https://doi.org/10.20900/immunometab20210008
Endlicher R, Drahota Z, Štefková K, Červinková Z, Kučera O (2023) The mitochondrial permeability transition pore—current knowledge of its structure, function, and regulation, and optimized methods for evaluating its functional state. https://doi.org/10.3390/cells12091273
Fontana-Ayoub M, Fasching M, Gnaiger E (2016) Selected media and chemicals for respirometry with mitochondrial preparations. https://wiki.oroboros.at/images/3/3c/MiPNet03.02_Chemicals-Media.pdf
Ghazal N, Kwong JQ (2025) Analyzing mitochondrial calcium influx in isolated mitochondria. https://doi.org/10.1007/978-1-0716-4164-4_12
Giorgi C, Marchi S, Pinton P (2018) The machineries, regulation and cellular functions of mitochondrial calcium. https://doi.org/10.1038/s41580-018-0052-8
Gnaiger E (2001) Bioenergetics at low oxygen: dependence of respiration and phosphorylation on oxygen and adenosine diphosphate supply. https://doi.org/10.1016/S0034-5687(01)00307-3
Gradl L, Gradl P, Gnaiger E (2021) Titration-injection microPump TIP2k manual. https://www.bioblast.at/images/9/9c/OroM2.3_TIP2k.pdf
Grynkiewicz G, Poenie M, Tsien RY (1985) A new generation of Ca^{2+} indicators with greatly improved fluorescence properties. https://www.jbc.org/article/S0021-9258(19)83641-4/pdf
Harisseh R, Abrial M, Chiari P, Al-Mawla R, Villedieu C, Tessier N, Bidaux G, Ovize M, Gharib A (2019) A modified calcium retention capacity assay clarifies the roles of extra- and intracellular calcium pools in mitochondrial permeability transition pore opening. https://doi.org/10.1074/jbc.RA119.009477
Komlodi T, Cardoso LHD, Doerrier C, Gnaiger E (2021) Coupling and pathway control of coenzyme Q redox state and respiration in isolated mitochondria. https://doi.org/10.26124/bec:2021-0003
Krumschnabel G, Eigentler A, Fasching M, Gnaiger E (2014) Use of safranin for the assessment of mitochondrial membrane potential by high-resolution respirometry and fluorometry. https://doi.org/10.1016/B978-0-12-416618-9.00009-1
Lassnig B, Gnaiger E (2010) Laboratory protocol: isolation of rat liver mitochondria. https://wiki.oroboros.at/images/9/93/MiPNet08.13_MitoIsolation-RLM.pdf

Li W, Zhang C, Sun X (2018) Mitochondrial Ca^{2+} retention capacity assay and Ca^{2+}-triggered mitochondrial swelling assay. https://doi.org/10.3791/56236

Liao J, Patel D, Zhao Q, Peng R, Guo H, Diwu Z (2021) A novel Ca^{2+} indicator for long-term tracking of intracellular calcium flux. https://doi.org/10.2144/btn-2020-0161

Makrecka-Kuka M, Krumschnabel G, Gnaiger E (2015) High-resolution respirometry for simultaneous measurement of oxygen and hydrogen peroxide fluxes in permeabilized cells, tissue homogenate and isolated mitochondria. https://doi.org/10.3390/biom5031319

Marchi S, Pinton P (2014) The mitochondrial calcium uniporter complex: molecular components, structure and physiopathological implications. https://doi.org/10.1113/jphysiol.2013.268235

McCormack JG, Halestrap AP, Denton RM (1990) Role of calcium ions in regulation of mammalian intramitochondrial metabolism. https://doi.org/10.1152/physrev.1990.70.2.391

Modesti L, Danese A, Vitto VAM, Ramaccini D, Aguiari G, Gafà R, Lanza G, Giorgi C, Pinton P (2021) Mitochondrial Ca^{2+} signaling in health, disease and therapy. https://doi.org/10.3390/cells10061317

Nászai A, Terhes E, Kaszaki J, Boros M, Juhász L (2019) Ca($^{2+}$)N it be measured? detection of extramitochondrial calcium movement with High-Resolution FluoRespirometry. https://doi.org/10.1038/s41598-019-55618-5

Picard M, Csukly K, Robillard ME, Godin R, Ascah A, Bourcier-Lucas C, Burelle Y (2008) Resistance to Ca^{2+}-induced opening of the permeability transition pore differs in mitochondria from glycolytic and oxidative muscles. https://doi.org/10.1152/ajpregu.90357.2008

Rizzuto R, De Stefani D, Raffaello A, Mammucari C (2012) Mitochondria as sensors and regulators of calcium signalling. https://doi.org/10.1038/nrm3412

Rottenberg H, Marbach M (1990) Regulation of Ca^{2+} transport in brain mitochondria. II. The mechanism of the adenine nucleotides enhancement of Ca^{2+} uptake and retention. https://doi.org/10.1016/0005-2728(90)90010-2

Saito A, Castilho RF (2010). Inhibitory effects of adenine nucleotides on brain mitochondrial permeability transition. https://doi.org/10.1007/s11064-010-0228-x

Scaduto RC, Grotyohann LW (1999) Measurement of mitochondrial membrane potential using fluorescent rhodamine derivatives. https://doi.org/10.1016/S0006-3495(99)77214-0

Serna JDC, Ramos VM, Cabral-Costa JV, Vilas-Boas EA, Amaral AG, Ohya G, Caldeira da Silva CC, Kowaltowski AJ (2022) Measuring mitochondrial Ca^{2+} efflux in isolated mitochondria and permeabilized cells. https://doi.org/10.26124/bec:2022-0007

Spinazzi M et al (2019) PARL deficiency in mouse causes Complex III defects, coenzyme Q depletion, and Leigh-like syndrome. https://doi.org/10.1073/pnas.1811938116

Thermo Fischer Scientific (2010) Indicators for Ca^{2+}, Mg^{2+}, Zn^{2+} and other metal ions. https://www.thermofisher.com/content/dam/LifeTech/global/technical-reference-library/Molecular%20Probes%20Handbook/chapter-pdfs/Ch-19-Ca-Mg-Zn-Ion-Indicators.pdf?icid=WE216841

Vercesi AE, Castilho RF, Kowaltowski AJ, de Oliveira HCF, de Souza-Pinto NC, Figueira TR, Busanello ENB (2018) Mitochondrial calcium transport and the redox nature of the calcium-induced membrane permeability transition. https://doi.org/10.1016/j.freeradbiomed.2018.08.034

Vilas-Boas EA, Cabral-Costa JV, Ramos VM, da Silva CCC, Kowaltowski A. (2023) Goldilocks calcium concentrations and the regulation of oxidative phosphorylation: Too much, too little, or just right. https://doi.org/10.1016/j.jbc.2023.102904

Vinnakota KC, Dash RK, Beard DA. (2011) Stimulatory effects of calcium on respiration and NAD(P)H synthesis in intact rat heart mitochondria utilizing physiological substrates cannot explain respiratory control in vivo. https://doi.org/10.1074/jbc.M111.242529

Williams SP, Fulton AM, Brindle KM (1993) Estimation of the intracellular free ADP concentration by fluorine-19 NMR studies of fluorine-labeled yeast phosphoglycerate

kinase in vivo. https://doi.org/10.1021/bi00069a026
Wollenman LC, Vander Ploeg MR, Miller ML, Zhang Y, Bazil JN (2017) The effect of respiration buffer composition on mitochondrial metabolism and function. https://doi.org/10.1371/journal.pone.0187523
Xu H, Ahn B, Van Remmen H (2022) Impact of aging and oxidative stress on specific components of excitation contraction coupling in regulating force generation. https://doi.org/10.1126/sciadv.add7377

Supplementary material

Table S1: *p*-values summarized from Figure 1a: ANOVA two-way with matching rows in the same experimental data and Tukey's multiple comparison post-test. Analyzed by GraphPad10.4.

Specific O_2 flux		MiRCa vs. MiR05	MiRCa+CaG vs. MiR05+CaG
1mt	*ren*	0.032	0.041
1PM	N_L	0.872	0.105
2D	N_P	0.312	0.016
2c	Nc_P	0.208	0.019
3G	N_P	0.068	0.697
4S	NS_P	0.823	0.621
5U	NS_E	0.922	0.878
6Rot	S_E	0.276	0.186
7Ama	*rox*	0.525	0.210

Table S2: *p*-values summarized from Figure 1b: ANOVA two-way with matching rows in the same experimental data and Tukey's multiple comparison post-test. Analyzed by GraphPad10.4.

FCR		MiRCa vs. MiR05	MiRCa+CaG vs. MiR05+CaG
1mt	*ren*	0.103	0.092
1PM	N_L	0.551	0.162
2D	N_P	0.592	0.006*
2c	Nc_P	0.555	0.002*
3G	N_P	0.412	0.992
4S	NS_P	0.668	0.277
5U	NS_E	-	-
6Rot	S_E	0.006*	0.006*
7Ama	*rox*	0.432	0.173

Footnote: the asterisks (*) indicate low *p*-values.

Table S3: Combined *p*-values summarized from Figure 1a, considering that CaG has no effect. Groups with CaG were integrated into the respective medium group. ANOVA two-way with matching rows in the same experimental data and Sidák's multiple comparison post-test. Analyzed by GraphPad10.4.

Specific O_2 flux		MiRCa and MiRCa+CaG vs. MiR05 and MiR05+CaG
1mt	*ren*	>0.999
1PM	N_L	>0.999
2D	N_P	0.996
2c	Nc_P	0.979
3G	N_P	0.736
4S	NS_P	0.009*
5U	NS_E	0.621
6Rot	S_E	0.010*
7Ama	*rox*	>0.999

Footnote: the asterisks (*) indicate low *p*-values.

Table S4: Combined *p*-values summarized from Figure 1b, considering that CaG has no effect. Groups with CaG were integrated into the respective medium group. ANOVA two-way with matching rows in the same experimental data and Sidák's multiple comparison post-test. Analyzed by GraphPad10.4.

FCR		MiRCa and MiRCa+CaG vs. MiR05 and MiR05+CaG
1mt	*ren*	0.998
1PM	N_L	0.999
2D	N_P	0.198
2c	Nc_P	0.038
3G	N_P	0.291
4S	NS_P	0.0002*
5U	NS_E	>0.999
6Rot	S_E	<0.0001*
7Ama	*rox*	>0.999

Footnote: the asterisks (*) indicate low *p*-values.

Standard calibration curve

Frequently, fluorescence calibrations are performed in experimental medium without sample (Picard et al 2008), but optical measurements are strongly influenced by suspended mitochondria (Grynkiewicz G et al 1985; Serna et al 2022). In the presence of sample, Ca^{2+} uptake must be inhibited. Figure S1a shows a representative trace of the calibration with sample in the presence of an inhibitor cocktail containing rotenone and antimycin A, and the uncoupler CCCP, to inhibit Ca^{2+} uptake. The second order polynomial fitting curve is shown in Figure S1b. In the range from 3 nA to 5.5 nA

(10 – 25 µM Ca^{2+}) the signal increased linearly, but less steeply at higher concentrations due to saturation of CaG.

We observed a shift of the calibration curves (Figure S1c) when comparing the calibration curve with and without sample. Therefore, the presence of sample is essential to perform a correct calibration.

Inhibiting Ca^{2+} uptake with the MCU inhibitor ruthenium red, RR, or inhibiting mitochondrial ETS and collapsing the protonmotive force *pmF* with the inhibitor cocktail containing rotenone and antimycin A, plus the uncoupler CCCP did not change the calibration curves (Figure S1d and S1e), except for one run (P7A, considered as an outlier). The first two Ca^{2+} titrations resulted in high variability of the change in the fluorescence signal (Δ*FS*) compared to the third and further titrations (Figure S1e). This can be explained by the variability of contaminant Ca^{2+} concentrations – since identical concentrations of EGTA were used in all experimental runs – and thus might not be related to the method of inhibiting Ca^{2+} uptake. Due to the difficulty of washing out the RR from the chambers, we recommend using the cocktail (Rot, Ama and CCCP), to avoid carry-over of RR to subsequent experiments. The more specific MCU inhibitor Ru360 can be considered but the carry-over was not evaluated in the present study. Of note, RR did not interfere significantly with the signal in the absence of mitochondria. Rot, Ama and CCCP were added after imt, allowing the sample's functionality to be assessed prior to inhibition. These compounds did not interfere with the CaG signal.

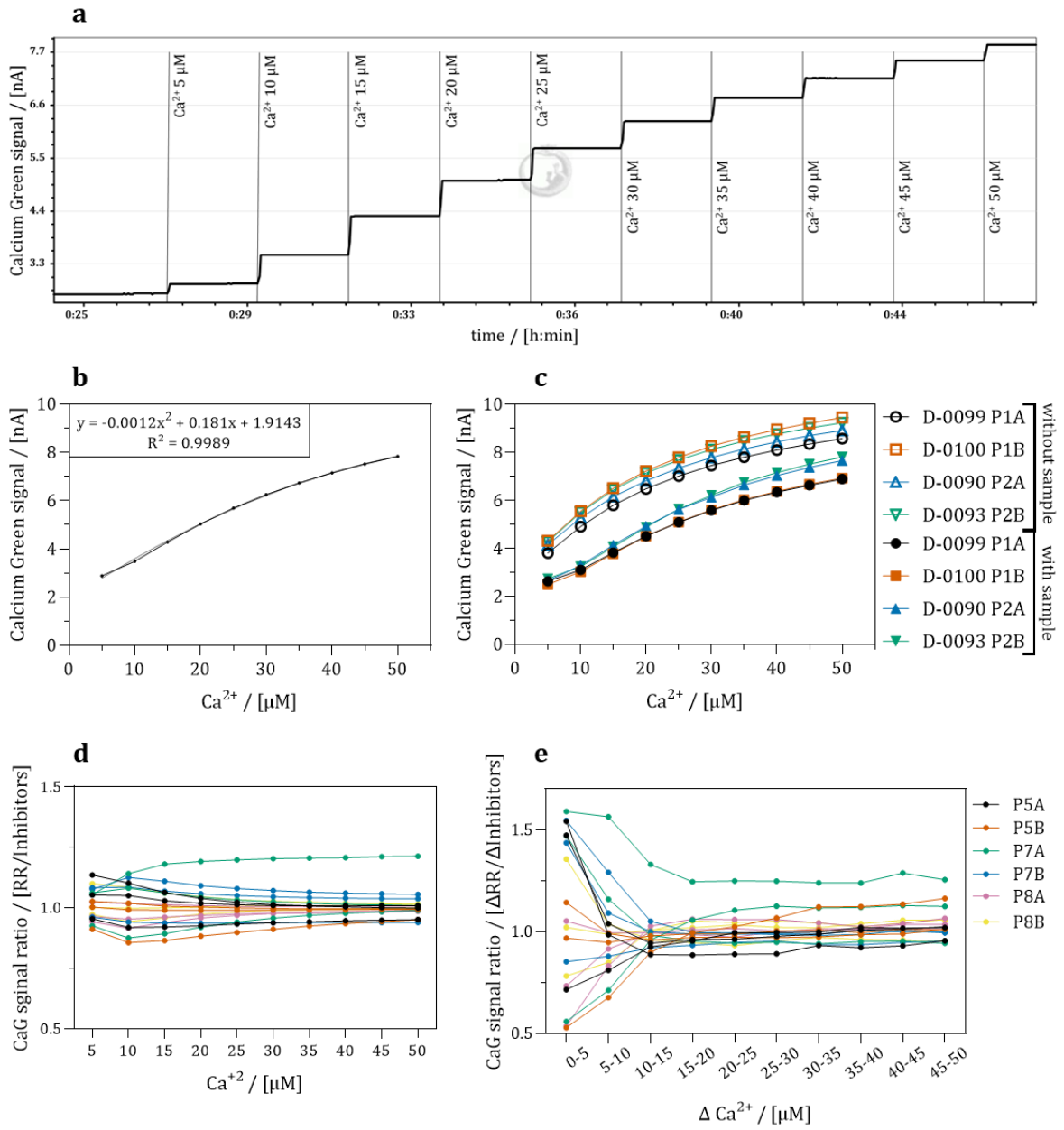

Figure S1. Calcium calibration in MiRCa (10 titrations of 5 µM $CaCl_2$ by TIP2k). Calibration was performed in the same conditions as the experiment, in the presence of liver mitochondria and RR or Rot+Ama+CCCP to inhibit Ca^{2+} uptake. **(a)** Representative trace of Calcium Green (CaG) signal in Ca^{2+} titrations. **(b)** Polynomial fit of the trace in panel a. Experiment: 2021-09-02 P3-03. **(c)** Polynomial fits in the absence or presence of sample and RR or Rot+Ama+CCCP to inhibit Ca^{2+} uptake. Identical combinations of chambers (P number and letters A and B for the right and left chamber, respectively) and Fluo-Sensors (D-number) were used under experimental conditions. Open and closed symbols indicate experiments without and with sample, respectively. **(d)** CaG signal ratio in response to 5 µM Ca^{2+} titrations in the presence of RR divided by the corresponding responses in the presence of Rot+Ama+CCCP (inhibitor cocktail). **(e)** ΔCaG signal ratio calculated as every Δ*FS* in the presence of RR divided by the corresponding Δ*FS* in the presence of Rot+Ama+CCCP. The same sample was used for calibration with RR or Rot+Ama+CCCP in 6 technical repeats on the same day (different colors) and the experiment was repeated on 3 different days (identical colors).

When comparing different samples using the same set of Fluo-Sensor and chamber, we observed that although there was slight difference at higher [Ca^{2+}] using the same set in combination 1 (Figure S2a), in combination 2 (Figure S2b) the CaG signal was comparable on different days with different samples.

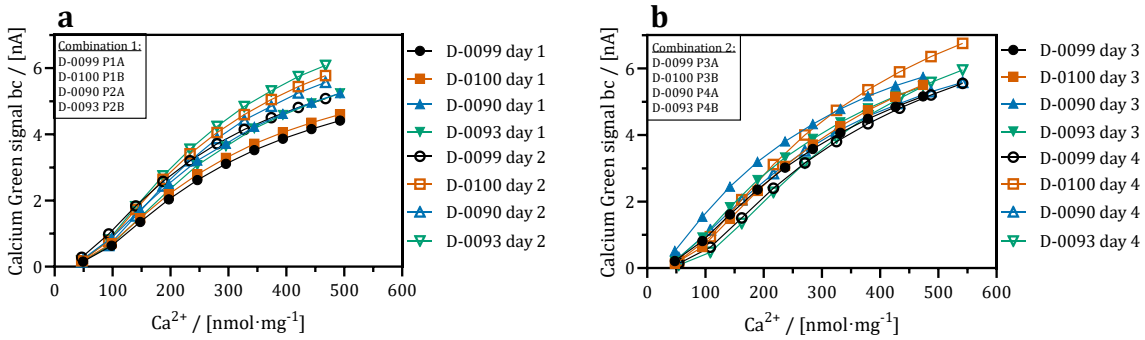

Figure S2. Influence of sample preparation on Ca^{2+} calibration. Calibrations were performed under experimental conditions, in the presence of isolated mitochondria from mouse liver with Ca^{2+} uptake inhibited by RR or Rot+Ama+CCCP. The same combination of chamber and Fluo-Sensor was used for comparison. **(a)** and **(b)** Polynomial fit baseline corrected for *rox* with different sample preparations performed on different days. Baseline day 1: 2.4529 ± 0.1070; day 2: 2.4159 ± 0.0986; day 3: 2.5506 ± 0.0881; day 4: 2.5521 ± 0.1159 (nA, median ± SD)